5.8 Conclusions

Stoichiometric and constraint-based modeling provides powerful methods for the characterization of, in particular, metabolic networks. It can form a basis for more detailed dynamical modeling of such systems. However, none of the approaches we discussed is able to adequately address all the potential applications of SNA (table 5.2).

Table 5.2 Approaches for stoichiometric network analysis, their requirements, and fields of application. Parentheses denote partial applicability.

	Constraints incorporated						
Approach	Stoichiometry	Thermodynamics	Quasi steady state	Reaction capacities	Optimality	**Computational costs**	**Flux distribution(s)**
Graph theory	(–)[a]	(+)	–	–	–	Low	None
CRs	+	–	–	–	–	Low	None
Kernel matrix	+	–	+	–	–	Low	All
MFA	+	(+)	+	(+)	–	Low	Single
FBA	+	+	+	+	+	Low	Single
MOMA	+	+	+	+	+	Medium	Single
EFMs/EPs	+	+	+	–	–	High	All

	Applications						
	Functional pathways	Optimal operation	Reaction importance	Reaction correlations	Pathway length	Network function	Robustness
Graph theory	–	–	(+)	(–)	(+)	(+)	(+)
CRs	–	–	–	–	–	–	–
Kernel matrix	–	–	–	(+)	–	(+)	–
MFA	–	–	(+)	–	–	–	–
FBA	–	+	(+)	–	–	+	(+)
MOMA	–	+	(+)	–	–	+	(+)
EFMs/EPs[b]	+	+	+	+	+	+	+

[a] Graph-theoretical methods use only connectivities and, possibly, directions.

[b] For the realistic case of equivalent sets of EPs and EFMs.

Hence, the methods for tackling a specific problem have to be carefully selected. More specifically, FBA and related approaches are most suitable for finding particular flux solutions even in genome-scale networks. Pathway analysis delivers a multitude of structural and functional aspects but is, in very large networks, hampered by combinatorial complexity. Despite such limitations, we expect the importance of SNA for systems biology to increase, particularly for an effective initial characterization of large-scale systems. We anticipate that the field will move towards a closer connection of the analysis of network structures in metabolism and regulation, which requires the development of new or modified theoretical methods.

6 Modeling Molecular Interaction Networks with Nonlinear Ordinary Differential Equations

Emery D. Conrad and John J. Tyson

Cellular processes, like growth, division, motility, and death, are controlled by complex networks of interacting macromolecules (genes, mRNAs, and proteins). These networks are sets of chemical reactions that convert reactant species into product species at rates that depend on reactant concentrations and, often, on the concentrations of other molecules (enzymes, inhibitors, transcription factors). To a first approximation, a reaction network can be described mathematically by a set of nonlinear ordinary differential equations that track the effects of these simultaneously occurring reactions. To gain some insight into the dynamical possibilities of such networks, we explore a set of increasingly more complicated network motifs, describing their effects in terms of signal-response curves. From our collection of simple functional motifs (buzzers, fuses, toggle switches, and a variety of oscillators) we can create realistic models of control systems actually employed by cells. As an example, we discuss the DNA-damage response pathway in mammalian cells.

6.1 Introduction

Molecular biologists often rely on suggestive cartoons to capture the complex interactions between many molecular components in functional networks of genes, proteins, and metabolites. In such cartoons (for example, figure 6.1), icons represent the interacting molecules and solid arrows their chemical transformations, for example, synthesis, degradation, phosphorylation, dephosphorylation, binding, and dissociation. Enzymatic and other indirect effects (such as allosteric activations or inhibition) are often represented by dashed arrows. These cartoons (or "wiring diagrams") are useful in summarizing many experimental observations, in capturing

the way biologists think about molecular mechanisms, and in suggesting new experiments to test or extend this molecular understanding of cell physiology.

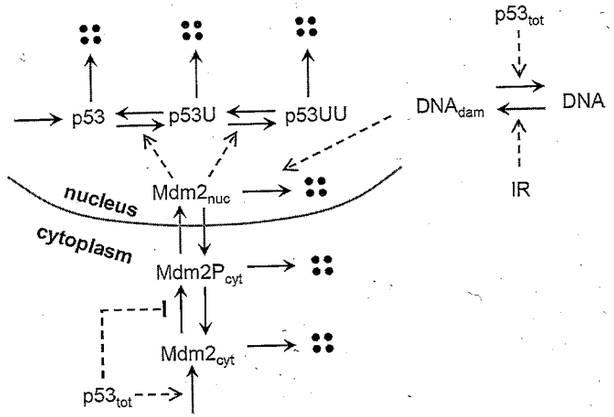

Figure 6.1 Example wiring diagram (reproduced from (Ciliberto et al., 2005), with permission). Intracellular proteins (p53, Mdm2, etc.) participate in a network of chemical reactions (solid arrows), such as synthesis, degradation, phosphorylation, and ubiquitination. Dashed arrows represent catalytic or regulatory effects on a reaction. This wiring diagram is a hypothetic mechanism (Ciliberto et al., 2005) for the interactions between p53, a transcriptional activator involved in cell cycle arrest and apoptosis, and Mdm2, a protein involved in degradation of p53. Mdm2 catalyzes the ubiquitination of p53, and polyubiquitinated p53 is rapidly degraded. Two feedback signals govern the behavior of the reaction network: (1) p53 stimulates the synthesis of Mdm2 in the cytoplasm, and (2) p53 indirectly inhibits the transport of Mdm2 into the nucleus. In response to DNA damage, the degradation of Mdm2 in the nucleus is upregulated. (IR = ionizing radiation)

Although most cell biologists use molecular wiring diagrams in these informal ways, we would like to pursue the idea that a reaction network is fundamentally a complex dynamical system and that its wiring diagram instructs how the concentrations of all the interacting components will change over time as the chemical reactions play out within the cell. From this point of view, the next question is how best to capture the dynamics of the network in mathematical form, in order to analyze and simulate its behaviors and ultimately to use the model to answer real physiological questions. For the purposes of this chapter, we will use nonlinear ordinary differential equations (ODEs) to represent the dynamical properties of reaction networks.

Realizing a reaction network as a system of ODEs is based on two assumptions. First, that our system is a "well-stirred" chemical reactor, so that component concentrations don't vary with respect to space. This is a reasonable assumption for cell-free extracts, but it hardly seems appropriate for an intact cell. Whether it is a good approximation or not depends on the time and space scales involved.

In box 6.1, we show that molecular diffusion is sufficiently fast to mix proteins throughout a yeast-sized cell in less than a minute. If we are interested in cell cycle processes (time scale = hours) or circadian rhythms (period = 1 day), then the "well-stirred" assumption is justified. If we are interested in membrane oscillations (time scale = seconds), then the "well-stirred" assumption would not be advisable.

When spatial information is required, then partial differential equations (PDEs) would be indicated. We will not discuss modeling by PDEs in this chapter, but note that, before one can appreciate the special properties of nonlinear PDE models (see chapter 9 of this book and Murray (2002b)), one must first master the principles in this chapter.

Box 6.1: How fast is molecular diffusion?
Given the typical diameter of a cell to be 10^{-3} cm and a typical diffusion constant for a protein in aqueous solution to be D=10^{-7}cm^2/s, we can calculate the average time for a protein to diffuse across a cell to be: $t = \frac{(10^{-3}cm)^2}{2\times10^{-7}cm^2/s} = 5s$. If diffusion is 10-fold slower in cytoplasm, then the average time to cross a cell is roughly 1 min. These are expected "mixing times" for macromolecules in cells. Metabolites (small molecules) will mix on a faster time scale.

The second basic assumption is that the variables (chemical concentrations) are continuous functions of time. This assumption is valid if the number of molecules of each species in the reaction volume (the cell or subcellular compartment) are sufficiently large (say, thousands of molecules each, at least). For concentrations greater than about 10 nM, we are safe using ODEs (see box 6.2).

Box 6.2: How many molecules of a regulatory protein in a cell?
A spherical cell of diameter 10^{-5} m has a volume of roughly 0.5×10^{-15} m^3 = 5×10^{-13} L. Given a typical concentration of a specific regulatory protein to be 10 nM, we calculate $10^{-8}\frac{\text{mol}}{\text{L}} \times 6 \times 10^{23}\frac{\text{molecules}}{\text{mol}} \times 5 \times 10^{-13}\ \frac{\text{L}}{\text{cell}}$=3,000 $\frac{\text{molecules}}{\text{cell}}$. For a reaction volume containing 3,000 molecules, we are justified in using ordinary differential equations to describe changes in a continuous variable $X(t)$ = concentration of species X. Were the concentration to drop below 1 nM, we would need to reformulate the model in terms of stochastic variables to capture the effects of molecular noise in the dynamical system.

If the total number of molecules of any particular substance, say, a transcription factor, is less than 1,000, then a stochastic differential equation or a Monte Carlo model would be more appropriate (Rao et al., 2002; McAdams and Arkin, 1999). Stochastic modeling is much more difficult than ODEs and requires a preliminary understanding of the deterministic dynamical system. For this reason, it makes sense to limit this chapter to ODE modeling and leave the harder stuff to chapter 8.

Granted these two simplifying assumptions, then ordinary differential equations are a very useful language in which to express mathematically the dynamical

consequences of a molecular interaction network. By applying a set of simple rules, we can express an arbitrarily complex reaction network as a set of coupled differential equations. The computer can then keep track of all the complex, interweaving interactions in the network and tell us with great precision what are the consequences of the mechanism that purports to describe some aspect of cell physiology. In this sense, kinetic modeling by differential equations is a tool for hypothesis testing (see chapter 1). If the mathematical consequences of the mechanism do not agree with observations, we must search for the problems in our hypotheses. If the consequences agree with the observations, then we can have some confidence that we are on the right track to understanding the mechanism.

We assume the reader has no familiarity with how to do kinetic modeling of chemical reactions beyond some vague (and possibly regretful) memories of the Michaelis-Menten equation. We start with the basic idea of using a simple rate law to describe how fast a chemical reaction proceeds and show how to estimate kinetic rate constants for isolated reactions from data. Then we assemble a few simple reactions (for protein synthesis, degradation, phosphorylation, and dephosphorylation) into modules for chemical buzzers, switches, and oscillators. These reaction motifs can then be linked together to form more complicated and realistic control systems. Writing the differential equations describing these systems can be largely automated, and solving the equations can be fully automated (see chapter 16). Fitting the results to experimental data and estimating rate constants are difficult tasks, which are the subjects of active research (chapter 11). We shall touch on all these issues in what follows.

6.2 Basic Building Blocks

6.2.1 From a Wiring Diagram to a Set of ODEs

To get from a wiring diagram to a set of ODEs, we must think about a network as a dynamical system whose state is changing from one moment of time to the next. We assign to each species (or icon) in the diagram a single *state variable*, $X(t)$ = the concentration of species X. The collection of values of all these variables $\{X_1(t), X_2(t), X_3(t), ...\}$ at any point in time constitutes the *state of the system*. Then, for each molecular species, we write a differential equation that describes how its concentration changes over time due to its interactions with the other species in the network. For example, for species X, we write

$$\frac{dX}{dt} = \text{synthesis} - \text{degradation} - \text{phosphorylation} + \text{dephosphorylation} - \text{binding} + \text{release, etc.} \quad (6.1)$$

The rate of each reaction (synthesis, degradation, etc.) must be represented by a *kinetic rate law*, which will have one or more *rate constants* associated with it. By assigning specific values to these rate constants, we fine-tune general rate laws to

particular reactions. The set of all rate constants needed to describe the reactions in a molecular interaction network is called the *parameter set* $\{p_1, p_2, \ldots p_m\}$ of the model.

In this paradigm, the dynamical consequences of a reaction network are determined by a system of nonlinear ordinary differential equations,

$$\frac{dX_i}{dt} = F_i(X_1, X_2, ..., X_n; p_1, p_2, ..., p_m), \; i = 1, 2, ..., n \quad (6.2)$$

The ODEs are nonlinear because the rate laws on the right-hand sides of equation 6.2 are often nonlinear functions of the state variables. Notice that the ODEs tell us how each state variable is *changing* with respect to time; they do not tell us the value of X at any specific time t. To solve the differential equations is to find these functions, $X_i(t)$, for each species (i) in the network. Each function corresponds to a measurable property of the system, the *time course* of species i. In order to solve equation 6.2 for the time courses $X_i(t)$, we must first prescribe a set of initial conditions $\{X_1(0), X_2(0), ..., X_n(0)\}$. The combination of rate equations, initial conditions, and parameter values is called a well-posed initial value problem (IVP), and its solution is guaranteed by a famous theorem stated informally in box 6.3.

Box 6.3: Existence and uniqueness theorem
Given very weak conditions on the smoothness of the rate laws on the right-hand side of equation 6.2, conditions that are usually satisfied by realistic models of reaction networks, the initial value problem has one and only one solution $\{X_1(t), X_2(t), ..., X_n(t)\}$ for all $0 \leq t < \infty$. By running time backwards, we can also find a unique prehistory of the system (for $-\infty < t \leq 0$).

Box 6.4: Linear and nonlinear differential equations
If the F_i's in equation 6.2 are linear functions of the variables, X_1, X_2, ..., X_n, then much can be said about the dynamical characteristics of the reaction system. The good news is that the solution can be expressed analytically in terms of exponential functions, $\exp(\lambda_i t)$, and harmonic functions, $\sin(\omega_i t + \phi_i)$. The bad news is that the dynamical possibilities of a linear system are very impoverished. In general, there can be only a single steady state solution, and all other solutions either approach this steady state as $t \to \infty$ or they blow up (some $X_j \to \infty$ as $t \to \infty$). Linear systems show none of the interesting dynamical behaviors (multiple steady states, limit cycle oscillations) to be described later in this chapter. The interesting dynamical features depend crucially on nonlinear dependencies of the F_i's on the X_j's.

We can imagine three types of "solutions" of a system of ODEs.

1. Analytical. Under very special circumstances (see, for example, box 6.4), it is possible to write the solution of a set of ODEs in terms of elementary functions,

such as $X_1(t) = X_1(0)e^{-k_a t}$, $X_2(t) = X_2(0)[1 + 0.5\sin(k_b t)]$, $X_3(t) = ...$, where $k_a, k_b, ...$ are rate constants and $X_1(0), X_2(0), ...$ are initial values.

2. Numerical. It is always possible to solve a well-posed IVP numerically on a computer. In principle, we can write

$$X_i(t + \Delta t) = X_i(t) + F_i(X_1(t), X_2(t), ..., X_n(t)) \cdot \Delta t \tag{6.3}$$

for each i. By starting at $X_i(0)$ and taking sufficiently small steps, Δt, we can "walk along" the time course to any time t in the future (or in the past). In practice, there are much more sophisticated, efficient, and accurate numerical schemes for walking along the time course (see chapter 16).

3. Qualitative. Whereas numerical integration of the ODEs gives us quantitative information about the solution (which is necessary if we are trying to account for quantitative experimental data), sometimes we are more interested in answers to qualitative questions, like, "What will the network do if I wait for a sufficiently long time?" (that is, characterize the solutions—the "stable attractors"—of the ODEs as $t \to \infty$) or "How will the long-term behavior of the network change if I double the rate of synthesis of protein X?" (that is, characterize the dependence of the stable attractors on any parameter in the ODEs).

To explore the examples that we will present, we suggest that the reader download XPPAUT or one of the other tools for simulating dynamical systems listed in the appendix.

Many of our qualitative methods depend on identifying and characterizing the steady state solutions of equation 6.2. A steady state solution is a set of constants $\{X_1^*, X_2^*, ..., X_n^*\}$ for which the net rate of change of every variable is zero, that is, $F_i(X_1^*, X_2^*, ..., X_n^*) = 0$ for all $i = 1, 2, ..., n$. A steady state is a special time-invariant solution of the ODEs, where the reactions producing and consuming each species perfectly cancel each other. Steady states can be either stable or unstable. Stable steady states attract all nearby solutions, whereas unstable steady states repel some nearby solutions as time increases.

6.2.2 Constant Synthesis

For starters, let's consider a constant rate of synthesis of some macromolecule, which can be described by the initial value problem $\frac{dX}{dt} = k_1$, $X(0) = X_0$. In this case, the differential equation is simple enough that we can guess the solution of the initial value problem: $X(t) = X_0 + k_1 t$. The numerical value of the rate constant must be estimated from experimental data. For example, from observations of accumulating cyclin in a frog egg extract (figure 6.2), we estimate that $k_1 = 1\text{nM/min}$.

$X(t) = X_0 + k_1 t$ is an example of an explicit, analytical solution. The uniqueness part of the theorem in box 6.3 assures us that once we have guessed a solution to the initial value problem, it is the only solution. We can sleep soundly at night, assured that we have not overlooked some other solution of this dynamical system.

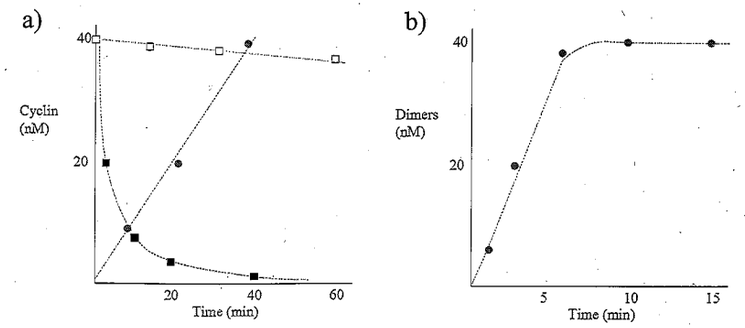

Figure 6.2 Experimental data used to estimate kinetic rate constants. a) Accumulation of cyclin (filled circles) in a frog egg extract; degradation of cyclin in interphase cells (open squares; (Felix et al., 1990)) and in metaphase cells (filled squares, from (Tang et al., 1993)). b) Formation of dimers of Cdk1 and cyclin B in an extract for which the initial concentration of Cdk1 monomers was approximately 100nM (Kumagai and Dunphy, 1995).

Once we have the solution, we can ask, "What happens to $X(t)$ as $t \to \infty$?" Well, it appears that the concentration of X grows without bound. We get this undesirable result because there is no term to counteract the growth rate in the differential equation.

6.2.3 Linear Degradation

Biochemical molecules naturally experience decay or degradation, and the rate at which this happens depends on how much of the molecule is present. In mathematical terms, $\frac{dX}{dt} = -k_2 X$, $X(0) = X_0$. The unique solution to this initial value problem is $X(t) = X_0 e^{-k_2 t}$. An interesting property of exponential decay is that X disappears with a constant half-life, $t_{1/2}$, defined by $X(t_{1/2}) = \frac{1}{2}X_0$. For linear degradation, $t_{1/2} = \frac{\ln 2}{k_2}$. From the data on cyclin degradation in figure 6.2, we see that cyclin is disappearing with a half-life of about 10 minutes, hence $k_2 \cong 0.07\ \text{min}^{-1}$.

At this point, the reader should consider what happens when we combine a constant rate of synthesis with linear degradation. That is, what is the analytical solution of the initial value problem: $\frac{dX}{dt} = k_1 - k_2 X$, $X(0) = X_0$? From the exact solution, show that $X(t) \to k_1/k_2$ as $t \to \infty$, for any $X_0 \geq 0$.

6.2.4 Autocatalytic Production

Autocatalysis is a process whereby a molecule activates its own production, either directly or indirectly through intermediates. In molecular biology, important examples include DNA synthesis and ribosome biogenesis. The simplest equation expressing autocatalysis is $\frac{dX}{dt} = k_2 X$. This is identical to the equation of the pre-

vious subsection, except for a difference of sign. The solution is $X(t) = X_0 e^{k_2 t}$. In this case, the solution grows with a constant *doubling time*, $t_2 = \frac{\ln 2}{k_2}$. We'll see more complex, indirect autocatalytic effects when we discuss feedback, later in the chapter.

6.2.5 Dimerization

Another fundamental reaction in biochemical networks is *dimerization*, where two species combine to form a complex. Examples include enzymes binding substrates, and the successive steps in the formation of hemoglobin, a four subunit heteromer ($\alpha_2\beta_2$). According to the Law of Mass Action, dimerization proceeds at a rate proportional to the product of the concentrations of the two binding species. Hence, we can express C binding X, forming the complex M, by the following scheme

reaction	C	+ X	→ M
initial concentrations	C_0	X_0	0
extent of reaction	-M	-M	M
concentrations at a later time	$C_0 - M$	$X_0 - M$	M

$$\frac{dM}{dt} = k_3 CX = k_3(C_0 - M)(X_0 - M)\ ,\ [k_3] = \frac{1}{\text{nM} \cdot \text{min}} \tag{6.4}$$

where we've chosen to write $C(t)$ and $X(t)$ in terms of $M(t)$ so that we have a single, solvable equation for the unknown function $M(t)$. The notation $[k_3]$ means "the units of k_3."

Now, guessing a solution to this equation requires a bit more imagination. Let's suppose that we receive a mysterious letter claiming that $M(t) = \frac{C_0 X_0(1-e^{-\alpha t})}{C_0 - X_0 e^{-\alpha t}}$, where $\alpha = k_3(C_0 - X_0)$, solves the initial value problem, when $M(0) = 0$, as in the scheme above. We can verify this claim by differentiating and doing a bit of algebra:

$$\frac{d}{dt}\left(\frac{C_0 X_0(1-e^{-\alpha t})}{C_0 - X_0 e^{-\alpha t}}\right) = \frac{\alpha C_0 X_0 (C_0 - X_0) e^{-\alpha t}}{(C_0 - X_0 e^{-\alpha t})^2} \tag{6.5}$$

and

$$\begin{aligned} k_3(C_0 - M)(X_0 - M) &= k_3 C_0 (1 - \frac{X_0(1-e^{-\alpha t})}{C_0 - X_0 e^{-\alpha t}}) X_0 (1 - \frac{C_0(1-e^{-\alpha t})}{C_0 - X_0 e^{-\alpha t}}) \\ &= \frac{\alpha C_0 X_0 (C_0 - X_0) e^{-\alpha t}}{(C_0 - X_0 e^{-\alpha t})^2} \end{aligned} \tag{6.6}$$

Remember that once we have a solution (even if it comes in the mail), it is the only solution we ever need (thanks to the existence and uniqueness theorem in box 6.3).

Notice from the analytical solution, $M(t) = \frac{C_0 X_0(1-e^{-\alpha t})}{C_0 - X_0 e^{-\alpha t}}$, where $\alpha = k_3(C_0 - X_0)$, that, if $C_0 > X_0$, then $\alpha > 0$ and $M(t) \to X_0$ as $t \to \infty$. On the other hand, if $C_0 < X_0$, then $\alpha < 0$ and $M(t) \to C_0$ as $t \to \infty$. In either case, the

asymptotic concentration of the complex is the initial concentration of the subunit in short supply. In principle, this conclusion is incorrect, because we have neglected dissociation of the complex (M → C + X, with some rate constant k_{-3}).

In order to estimate the rate constant from the data in figure 6.2b, we notice that $C_0 = 100$ nM and $X_0 \cong 40$ nM (why?). Considering that it takes about 3 minutes for $M(t)$ to reach 20 nM, we can solve $M(3) = 20$ for α:

$$M(3) = \frac{4000(1-e^{-3\alpha})}{100 - 40e^{-3\alpha}} = 20 \tag{6.7}$$

$$\Rightarrow \quad 200 - 200e^{-3\alpha} = 100 - 40e^{-3\alpha} \tag{6.8}$$

$$\Rightarrow \quad \frac{5}{8} = e^{-3\alpha} \ \Rightarrow \ \alpha = \frac{1}{3}\ln\frac{8}{5}\ \text{min}^{-1} \tag{6.9}$$

Therefore, we estimate that $k_3 = \frac{1}{180}\ln\frac{8}{5}\text{nM}^{-1}\text{min}^{-1} = 2.6 \times 10^{-3}\text{nM}^{-1}\text{min}^{-1}$.

6.2.6 Michaelis-Menten Kinetics

The diagram in figure 6.3a represents the enzymatic transformation of substrate X into product P. Michaelis and Menten (1913) and Briggs and Haldane (1925) first explored the elementary reaction mechanism (figure 6.3b) for this process. Assuming that the total enzyme concentration E_T is much less than the initial substrate concentration, X_0, they showed that the rate of the enzyme-catalyzed reaction can be written as: $\frac{dX}{dt} = -\frac{dP}{dt} = \frac{-k_2 E_T X}{K_m + X}$, where $K_m = \frac{k_{-1}+k_2}{k_1}$ is called the Michaelis constant. Note that $[K_m]$ = nM. A rigorous derivation of the Michaelis-Menten rate law can be found in (Murray, 2002a), and in (Segel, 1988).

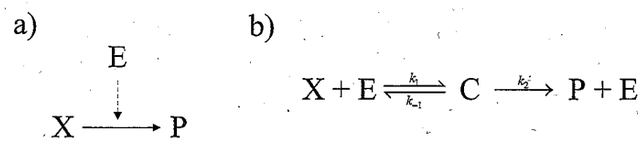

Figure 6.3 Michaelis-Menten kinetics. a) Enzyme E catalyzes the conversion of substrate X into product P. b) Michaelis-Menten mechanism for an enzyme-catalyzed reaction: E binds the substrate X to form a complex C; in the complex, E converts X to P; once the conversion is done, E dissociates from P and is free to bind another molecule of substrate.

Among other things, the Michaelis-Menten rate law can be used to reduce the number of variables which describe a typical enzymatic conversion process, such as phosphorylation or dephosphorylation. This reduction is often useful when trying to understand the dynamic possibilities of a network using analytical and qualitative methods. On the other hand, one must keep in mind the assumption ($E_T \ll X_0$) so that the rate law is applied in a consistent fashion.

6.3 Simple Networks and Signal-Response Curves

The basic rate laws just described can be combined to form reaction motifs that are commonly found in biochemical networks. These motifs have specific characteristics that dominate their behavior within larger networks. In order to build some dynamical intuition that may be useful in understanding larger, more realistic macromolecular networks, we first explore the properties of some common network motifs.

6.3.1 Synthesis and Degradation

Our first motif is simultaneous synthesis and degradation (figure 6.4a), described by $\frac{dX}{dt} = k_1 S - k_2 X$, with $X(0) = 0$. In this equation, we might think of S ("signal") as the concentration of mRNA encoding protein X. Notice that $[k_1] = [k_2] = \text{min}^{-1}$. The solution of this ODE, which was posed as a problem earlier in the chapter, is $X(t) = \frac{k_1 S}{k_2}(1 - e^{-k_2 t})$. Notice that as $t \to \infty$, $e^{-k_2 t} \to 0$, and our solution tends towards the value $X_{ss} = \frac{k_1 S}{k_2}$. Notice also that $k_1 S - k_2 X_{ss} = 0$, so X_{ss} is the steady state solution of the differential equation, as described earlier.

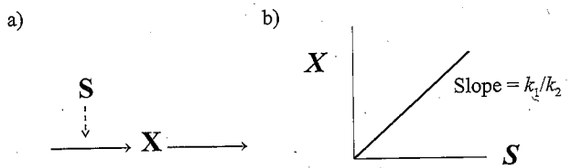

Figure 6.4 A signal-response relationship. a) Signal S stimulates the synthesis of protein X. b) Linear response of steady state protein concentration to signal strength.

If we think of S as an input signal (mRNA concentration) and X as the response (protein concentration), then this motif at steady state generates a *linear signal-response curve*, as depicted in figure 6.4b.

6.3.2 Phosphorylation and Dephosphorylation

Now suppose X is phosphorylated and dephosphorylated as depicted in figure 6.5a. Choosing to model both the forward and reverse steps using simple linear kinetics, we write $\frac{dX_P}{dt} = k_1 S(X_T - X_P) - k_2 X_P$, where X_T is the total concentration of both phosphorylated and unphosphorylated forms of X (so that $X_T - X_P = X$), and S is the concentration of the protein kinase. (The concentration of the protein phosphatase is absorbed into the value of k_2.) Notice that $[k_1] = \text{nM}^{-1}\,\text{min}^{-1}$, $[k_2] = \text{min}^{-1}$. Solving $\frac{dX_P}{dt} = 0$ results in a single steady state solution, $X_{P,ss} = \frac{X_T S}{(k_2/k_1)+S}$, which is a hyperbolic function of S(see figure 6.5b). This is called a *hyperbolic signal-response curve.*

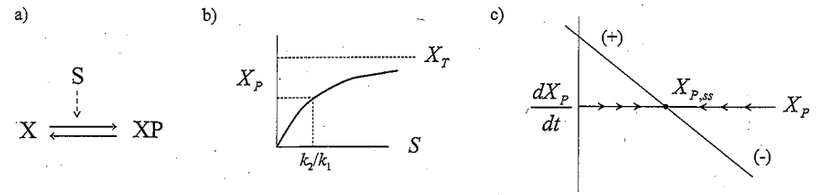

Figure 6.5 Hyperbolic signal-response curve (see text).

We can determine the stability of the steady state graphically by plotting $\frac{dX_P}{dt}$ as a function of X_P. Noting that trajectories lie along the x-axis, we see that for $\frac{dX_P}{dt} > 0$ (that is, wherever the curve is above the x-axis), the solution, $X_P(t)$, moves to the right along the x-axis and for $\frac{dX_P}{dt} < 0$ (where the curve is below the x-axis), the solution moves to the left. The curve crosses the x-axis at $X_{P,ss}$, the steady state. The stability of the steady state is then obvious because $X_P(t)$ moves towards $X_{P,ss}$ along the x-axis (figure 6.5c). This method of determining stability can be applied to any single-variable system.

Our assumption of linear kinetic rate laws implies that X_T is much less than the Michaelis constants of both the kinase and the phosphatase. If this is not the case, then we should use Michaelis-Menten rate laws.

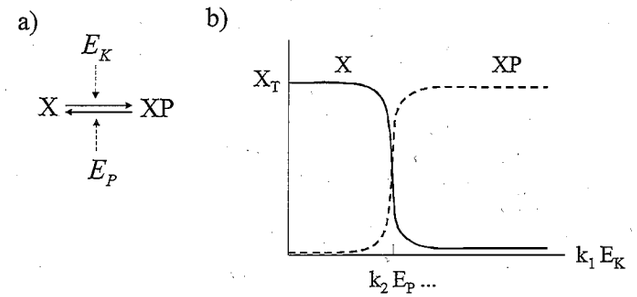

Figure 6.6 Sigmoidal signal-response curve (see text).

In this case (figure 6.6a), the governing ODE is

$$\frac{dX}{dt} = -\frac{k_1 E_K X}{K_{m1} + X} + \frac{k_2 E_P (X_T - X)}{K_{m2} + X_T - X}, \tag{6.10}$$

where $X_T - X = X_P$, E_K and E_P are the total concentrations of kinase and phosphatase (taken to be constant in this equation), and K_{m1} and K_{m2} are the Michaelis constants. At steady state, we have

$$\frac{k_1 E_K X}{K_{m1} + X} = \frac{k_2 E_P (X_T - X)}{K_{m2} + X_T - X} \tag{6.11}$$

or, after simplifying and scaling the relevant variables,

$$u_1 x(J_2 + 1 - x) = u_2(1 - x)(J_1 + x) \tag{6.12}$$

where $x = X/X_T$, $u_1 = k_1 E_K$, $u_2 = k_2 E_P$, $J_1 = K_{m1}/X_T$, $J_2 = K_{m2}/X_T$. Using the quadratic formula, we can solve this equation for x as a function of u_1, u_2 , J_1, and J_2. We get $x = G(u_1, u_2, J_1, J_2)$, where the *Goldbeter-Koshland* function, G, is defined as

$$G(u_1, u_2, J_1, J_2) = \frac{2u_1 J_2}{B + \sqrt{B^2 - 4(u_2 - u_1)u_1 J_2}} \tag{6.13}$$

where $B = u_2 - u_1 + u_2 J_1 + u_1 J_2$ (see Goldbeter and Koshland (1981)). In terms of the original variables, X_{ss} is a sigmoidal function of the input signal E_K (see figure 6.6b), and so we call this a *sigmoidal signal-response curve*. The sigmoid becomes more and more switch-like as J_1 and J_2 become much less than 1.

To confirm the sigmoidal character of the Goldbeter-Koshland function, it is easier to think of u_1 as a function of x than x as a function of u_1. Rearranging equation 6.12, we find that $u_1 = u_2 \frac{J_1+x}{J_2+1-x} \cdot \frac{1-x}{x}$. As a function of x, this curve crosses the x-axis at $x = 1$ and $x = -J_1$ and has vertical asymptotes at $x = 0$ and $x = 1 + J_2$. For $0 < J_1, J_2 \ll 1$, the curve must have the shape illustrated in figure 6.6b.

We can prove the stability of the steady state by the same graphical methods used for the case of linear reaction kinetics, but we omit the details.

6.4 Networks with Feedback

6.4.1 What Is Feedback?

Biochemical reaction networks commonly contain feedback loops, for which the output of one reaction affects the progress of an upstream reaction. Feedback can be characterized as positive or negative, depending on the net effect of the interactions. When reaction networks have intertwined feedback loops, their dynamical properties can be exceedingly complex (see chapter 1 and chapter 2).

We start our investigation of feedback loops with two-component interactions (figure 6.7), which can be categorized as negative feedback (6.7a and b), positive feedback (6.7c), or mutual antagonism (6.7d). Mathematically speaking, the effect of species X_j on the rate of change of another species X_i, $\frac{dX_i}{dt} = F_i(X_1, ..., X_n)$, is the partial derivative $\frac{\partial F_i}{\partial X_j}$. The sign of this derivative determines whether the feedback is positive or negative. Naturally, this partial derivate need not be constant and may change sign based on the state and on parameter values, so classifying the effect isn't always unambiguous. A chain of such effects makes a feedback loop if it starts and ends with the same species.

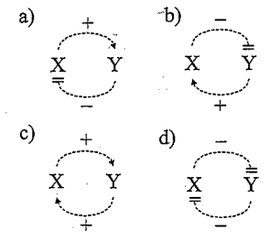

Figure 6.7 Three types of feedback are possible between two components: a) and b) are negative feedback, c) positive feedback, d) mutual antagonism.

6.4.2 Negative Feedback

We start with a simple example of negative feedback (figure 6.8). The phosphorylated form of Y activates the degradation of X, and X is the kinase that phosphorylates Y. In this case, we need at least two differential equations to characterize the system:

$$\frac{dX}{dt} = k_1 S - k_2 Y_P X \tag{6.14}$$

$$\frac{dY_P}{dt} = \frac{k_3 X(Y_T - Y_P)}{K_{m3} + Y_T - Y_P} - \frac{k_4 E Y_P}{K_{m4} + Y_P} \tag{6.15}$$

where $Y = Y_T - Y_P$ is the concentration of the unphosphorylated form of Y, $[X] = [Y_P] = [S] = [E] =$ nM, $[k_1] = [k_3] = [k_4] = \text{min}^{-1}$, $[k_2] = \text{nM} \cdot \text{min}^{-1}$, and $[K_{m3}] = [K_{m4}] =$ nM. The equation for X is constant synthesis (proportional to S) minus degradation (proportional to $Y_P \cdot X$). The equation for Y_P is just the case studied in the subsection 6.3.2. We know how each of these differential equations behaves in isolation, but what happens when they are coupled together?

6.4.3 Phase Planes, Vector Fields, and Nullclines

As described earlier, at any point in time t_0, the network must reside in a particular state, $(X(t_0), Y(t_0))$, which is just a point in the two-dimensional *state space* of the system of ODEs. For the case of a two-species network, the state space is called the *phase plane*. At each point in the phase plane, the differential equations define a vector that tells us which direction and how far the dynamical system will move over the next small increment of time, Δt. We can think of the phase plane as covered with little vectors, like the hair on the head of a new military recruit. This collection of vectors is called the *vector field*. A solution to the ODEs is just a curve that starts at some initial point and follows the vector field.

The vector field in the phase plane is conveniently characterized by the X- and Y-nullclines, the curves for which the corresponding species' time derivative is exactly zero. Along the X-nullcline, the vector field points north (N) or south (S) because $\frac{dX}{dt} = 0$ (that is, no change in the east-west direction). Along the Y-nullcline,

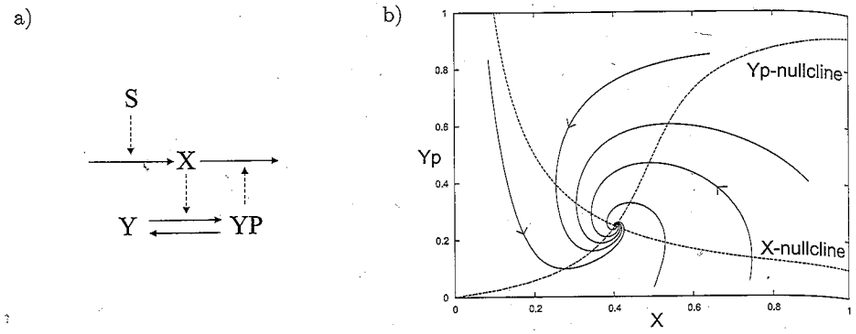

Figure 6.8 Example of negative feedback. a) Wiring diagram. b) Phase portrait. Dashed curves: nullclines given by equations 6.16 and 6.17; solid curves: trajectories of equations 6.14 and 6.15. Parameter values are $k_1 = k_2 = k_3 = k_4 = 1$, $S = K_{m3} = K_{m4} = 0.1$, $Y_T = 1$, and $E = 0.5$. In b), trajectories spiral into a stable steady state at the intersection of the nullclines.

the vector field points east (E) or west (W) because $\frac{dY}{dt} = 0$ (no change in the north-south direction). In the region between the nullclines, the vector field adopts one of four characteristic compass directions (NE, SE, SW, or NW). Wherever the nullclines intersect, the pair of ODEs has a steady state solution (both $\frac{dX}{dt} = 0$ and $\frac{dY}{dt} = 0$).

In the above example for negative feedback, the nullclines are:

$$\text{X-nullcline:} \qquad k_1 S = k_2 Y_P X \Rightarrow Y_P = \frac{k_1 S}{k_2 X} \tag{6.16}$$

$$\text{Yp-nullcline:} \qquad \frac{k_3 X(Y_T - Y_P)}{K_{m3} + Y_T - Y_P} = \frac{k_4 E Y_P}{K_{m4} + Y_P}$$

$$\Rightarrow \qquad Y_P = Y_T \cdot G(k_3 X, k_4 E, \frac{K_{m3}}{Y_T}, \frac{K_{m4}}{Y_T}) \tag{6.17}$$

where G is the Golbeter-Koshland function defined by equation 6.13. These curves are easily plotted on the phase plane (figure 6.8b) along with representative trajectories that point out how the system evolves with time given several different initial conditions. The X-nullcline is a hyperbola, while the Y_P-nullcline is a sigmoidal curve with the switch point at $X = \frac{k_4 E}{k_3} \cdot \frac{Y_T + 2K_{m3}}{Y_T + 2K_{m4}}$. Of particular note is how all trajectories seem to be sucked into the steady state. When this is the case, we call the steady state locally and globally stable. It is possible to be locally stable but not globally stable or to be locally unstable, as we shall soon see.

6.4.4 Positive Feedback

Figure 6.9 presents a simple example of positive feedback, where species X activates species Y (via phosphorylation) and the phosphorylated form of Y promotes the synthesis of X.

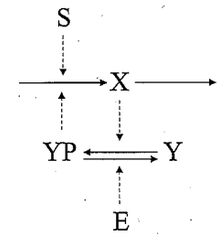

Figure 6.9 Example of positive feedback. Wiring diagram.

One possible set of equations to describe this network is

$$\frac{dX}{dt} = k_1 S + k_2 Y_P - k_3 X \tag{6.18}$$

$$\frac{dY_P}{dt} = \frac{k_4 X(Y_T - Y_P)}{K_{m4} + Y_T - Y_P} - \frac{k_5 E Y_P}{K_{m5} + Y_P} \tag{6.19}$$

where $[X] = [Y_P] = [S] = [E] = \text{nM}$, $[k_1] = [k_2] = [k_3] = [k_4] = [k_5] = \text{min}^{-1}$, and $[K_{m4}] = [K_{m5}] = \text{nM}$. For this system of equations, the X-nullcline is $Y_P = (k_3/k_2)X - k_1 S$ and the Y_P-nullcline is $Y_P = Y_T \cdot G(k_4 X, k_5 E, K_{m4}/Y_T, K_{m5}/Y_T)$ (plotted in figure 6.10a). Notice that as we increase or decrease S, the X-nullcline moves down or up, and there is a range of S values, $S \in (S_{c1}, S_{c2})$, for which the nullclines intersect in three places. The points at the end of this range, where the system changes from one to three steady states, are called saddle-node (SN) bifurcation points. For $S_{c1} < S < S_{c2}$, we say that the system is *bistable*.

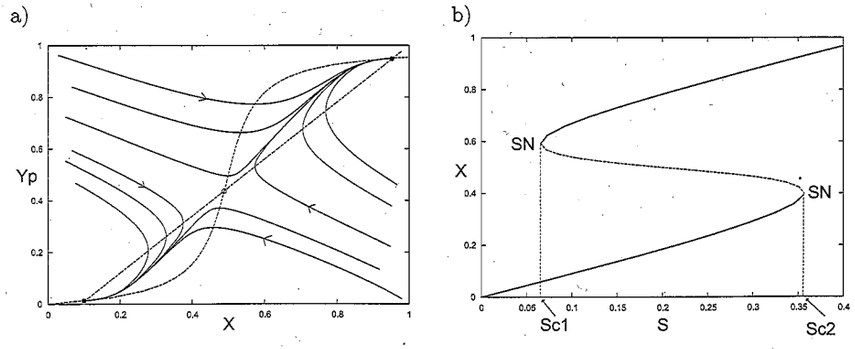

Figure 6.10 Example of positive feedback. a) Phase portrait. b) One parameter bifurcation diagram. Solid curves: stable steady states; dashed curve in between: unstable steady states. For $S_{c1} < S < S_{c2}$, the control system is bistable. Parameter values are $k_1 = k_4 = 1$, $k_2 = 0.8$, $k_3 = 1.2$, $S = 0.2$, $K_{m3} = K_{m4} = 0.05$, $Y_T = 1$, and $E = 0.5$. In a), trajectories move away from the unstable steady state (in the center) to one of two stable steady states.

A good way to visualize this bifurcation behavior is to plot a one parameter bifurcation diagram with S on the abscissa and either the X or YP concentration for each steady state on the ordinate, as in figure 6.10b. In general, this is a compact way to visualize how the dynamics of a system depend on its parameters. In this particular case, the system exhibits hysteresis as the parameter S passes back and forth through the region of bistability. That is, for low S, the system is at rest in the lower steady state (which is globally attracting). As S increases, the control system remains at this lower steady state, even after passing into the region of bistability because the lower steady state is stable with respect to small perturbations. Finally, as S increases past the upper bifurcation point (S_{c2}), the system abruptly shifts to the upper stable steady state. Now, if S were to decrease, the control system would remain in the upper steady state until S falls below the lower critical value, S_{c1}. Only then will the system switch back to the lower steady state. This non-reversibility is called *hysteresis*.

6.4.5 Mutual Antagonism

Mutual antagonism is a situation where an increase in either species means a decrease in the other, as in figure 6.11. Here, X phosphorylates Y, so more X implies less Y. Further, Y degrades X, so more Y means less X. The equations for this module are:

$$\frac{dX}{dt} = k_1 S - (k_2' + k_2 Y)X \tag{6.20}$$

$$\frac{dY}{dt} = \frac{k_3 E(Y_T - Y)}{K_{m3} + Y_T - Y} - \frac{k_4 XY}{K_{m4} + Y} \tag{6.21}$$

where $Y_T = Y + Y_P$ is constant, and the dimensions of the variables and rate constants are as before. In this case, the X-nullcline is now a hyperbola $Y = \frac{k_1 S - k_2' X}{k_2 X}$, which is similar to the negative feedback case. The Y-nullcline is $Y = Y_T \cdot G(k_3 E, k_4 X, K_{m3}/Y_T, K_{m4}/Y_T)$, which is a switch function that turns off as X increases. As in the case of positive feedback, there may be multiple intersections of the nullclines and a region of bistability for the parameter S (see figure 6.12a). Figure 6.12b shows a one-parameter bifurcation diagram for this system.

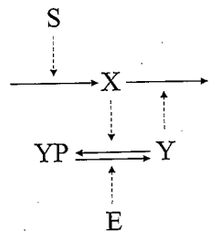

Figure 6.11 Example of mutual antagonism. Wiring diagram.

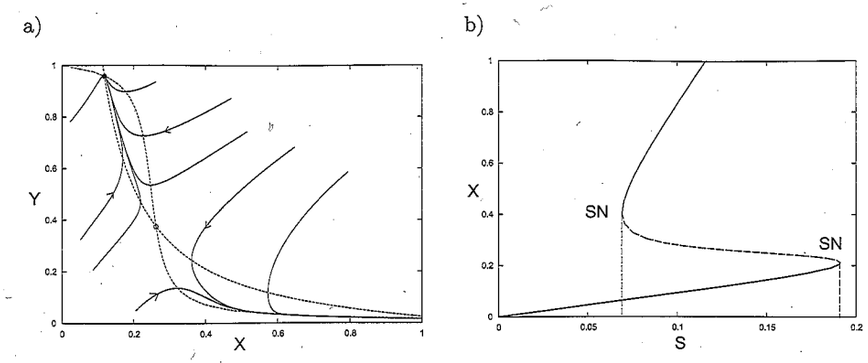

Figure 6.12 Example of mutual antagonism. a) Phase portrait. b) One parameter bifurcation diagram. Parameter values are $k_1 = k_2 = k_3 = k_4 = 1$, $k_2' = 0.1$, $S = 0.125$, $K_{m3} = K_{m4} = 0.05$, $Y_T = 1$, and $E = 0.25$. In a), trajectories move away from the unstable steady state (in the center) to one of two stable steady states.

Recently there have appeared a number of interesting experimental studies of bistability in macromolecular regulatory networks: in the MAP kinase signaling pathway of frog eggs (Ferrell Jr. and Machleder, 1998; Xiong and Ferrell Jr., 2003), in the activation of MPF in frog egg extracts (Sha et al., 2003; Pomerening et al., 2003), in the lactose utilization network of bacteria (Ozbudak et al., 2004), and in artificial genetic networks (Gardner et al., 2000).

6.5 Networks That Oscillate

There are three simple motifs that generate oscillatory behavior: activator-inhibitor, substrate-depletion, and delayed negative feedback.

6.5.1 Activator-Inhibitor

In figure 6.13, R stimulates its own production by phosphorylating E, and E_P also stimulates the production of X. (Think of E_P as the active form of a transcription factor.) As X increases, it promotes degradation of R. This negative feedback loop between X and R can cause oscillation (figure 6.14a). The equations for this system are

$$\frac{dR}{dt} = k_0 E_p + k_1 S - k_2 XR \tag{6.22}$$

$$\frac{dX}{dt} = k_3 E_p - k_4 X \tag{6.23}$$

where $E_p = E_T \cdot G(k_5 R, k_6, \frac{K_{m5}}{E_T}, \frac{K_{m6}}{E_T})$. The X-nullcline is $X = (k_3/k_4)E_p$ and the R-nullcline is $X = (k_0 E_p + k_1 S)/k_2 R$. The phase portrait (figure 6.14a) clearly shows the tendency of the vector field to drive trajectories in a circulatory pattern. For

appropriate values of the parameters, the control system exhibits a closed trajectory, called a stable limit cycle. As the system rotates around the limit cycle, $R(t)$ and $X(t)$ oscillate periodically in time. The classic example of activator-inhibitor oscillations in cell biology is the cyclic AMP signaling system of the cellular slime mold, *Dictyostelium discoideum* (Martiel and Goldbeter, 1987); see box 6.5.

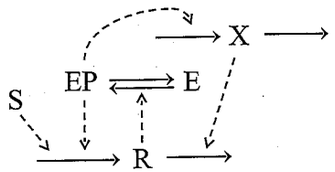

Figure 6.13 An activator-inhibitor oscillator. Wiring diagram.

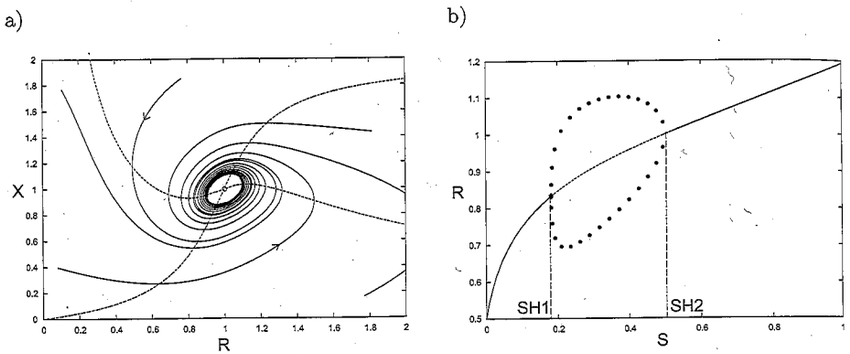

Figure 6.14 An activator-inhibitor oscillator. a) Phase portrait, b) One parameter bifurcation diagram. Parameter values are $k_0 = k_1 = k_2 = k_3 = k_5 = k_6 = 1$, $k_4 = 0.5$, $S = 0.5$, $K_{m5} = K_{m6} = 0.1$, and $E_T = 1$. In a), trajectories spiral in towards a limit cycle surrounding the unique unstable steady state. In b), the min and max values of R on the limit cycle oscillation are plotted in the region between the two Hopf bifurcations, S_{H1} and S_{H2}.

As we increase or decrease the signal strength, S, the R-nullcline shifts up or down, and though there is always only one steady state (one intersection of the nullclines), the stability of the steady state changes as we change S. For $S_{H1} < S < S_{H2}$, the steady state is unstable and surrounded by a limit cycle. The boundary points, S_{H1} and S_{H2}, are called Hopf bifurcation points. Figure 6.14b plots the one-parameter bifurcation diagram for this system, along with the amplitude of the oscillatory solution where it exists.

Box 6.5: Cyclic AMP oscillations in *Dictyostelium*
Cyclic AMP binds to a membrane receptor, which activates adenylate cyclase, the enzyme that catalyzes the synthesis of cyclic AMP from ATP (this is the positive feedback loop promoting the autocatalytic production of cyclic AMP). Meanwhile, cyclic AMP binding to the receptor promotes phosphorylation and desensitization of the receptor (this is the negative feedback loop, the desensitized receptor being the "inhibitor" that shuts off autocatalytic production of cyclic AMP). Next, cyclic AMP is hydrolyzed to 5'-AMP, which allows the receptor to slowly regain its sensitivity. Only then can there be a new burst of cyclic AMP synthesis.

6.5.2 Substrate-Depletion

In the substrate-depletion motif (figure 6.15), substrate X is converted by enzyme E into product R in a process which is autocatalytically amplified by R-dependent phosphorylation of E. This positive feedback loop leads to an explosive production of R which depletes the pool of the substrate, X. Naturally, once X is depleted, the production of R ceases and the degradation of R reduces its concentration below the level necessary to sustain the positive feedback loop. At this point, the pool of X begins to replenish. When X builds up sufficiently high, the positive feedback loop reengages, and a new burst of R synthesis commences.

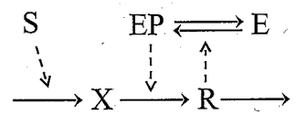

Figure 6.15 A substrate-depletion oscillator. Wiring diagram.

The differential equations for the model in figure 6.15 are

$$\frac{dX}{dt} = k_1 S - (k_0' + k_0 E_p)X \tag{6.24}$$

$$\frac{dR}{dt} = (k_0' + k_0 E_p)X - k_2 R \tag{6.25}$$

where $E_p = E_T \cdot G(k_3 R, k_4, \frac{K_{m3}}{E_T}, \frac{K_{m4}}{E_T})$. The X-nullcline is $X = \frac{k_1 S}{(k_0' + k_0)E_p}$ and the R-nullcline is $X = \frac{k_2 R}{(k_0' + k_0)E_p}$. Again, the phase portrait (figure 6.16a) shows a circulatory pattern around the steady state, and for a suitable choice of parameters, the system executes a stable limit cycle oscillation. In this case, the X-nullcline shifts upward (downward) as S increases (decreases). As before, the one-parameter bifurcation diagram shows two Hopf bifurcations and oscillatory solutions in between (figure 6.16b). Substrate-depletion oscillations are common in biochemical networks (see table 6.1).

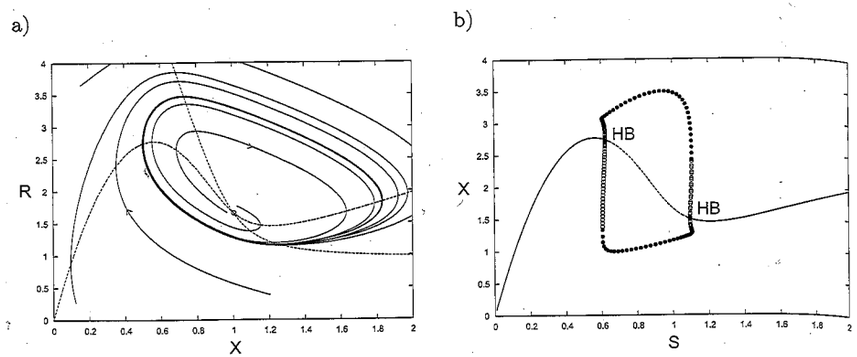

Figure 6.16 A substrate-depletion oscillator. a) Phase portrait. b) One parameter bifurcation diagram. Parameter values are $k_0 = k_1 = k_2 = k_3 = k_4 = 1$, $k_0' = 0.1$, $S = 1$, $K_{m3} = K_{m4} = 0.1$, and $E_T = 1$. In a), trajectories spiral in towards a limit cycle surrounding the unique unstable steady state. In b), the min and max values of X on the limit cycle oscillation are plotted in the region between the two Hopf bifurcations.

Table 6.1 Examples of substrate-depletion oscillators.

Example	Substrate	Activator	Reference
Frog egg	Cyclin B	MPF	(Tyson, 1991)
Glycolysis	F6P+ATP	FDP+ADP	(Selkov, 1968)
Calcium	Ca^{2+} in ER[a]	Ca^{2+} in cytosol	(Dupont et al., 1991)
Ecosystem	Prey	Predator	(Maynard-Smith, 1974)

[a] ER = endoplasmic reticulum.

6.5.3 Delayed Negative Feedback

In figure 6.17, we present an example of delayed negative feedback. In this scheme, R phosphorylates E, which then binds to C to form X, and X is the active complex that degrades R itself (closing the negative feedback loop). This motif is derived from components of the cell cycle regulatory mechanism in eukaryotes, where R is MPF (mitosis promoting factor), E is APC (anaphase promoting complex), C is Cdc20, and X is a complex of APC and Cdc20.

The corresponding set of equations is

$$\frac{dR}{dt} = k_1 S - k_2 X R \tag{6.26}$$

$$\frac{dE_P}{dt} = \frac{k_3 R(E_T - E_P)}{K_{mk} + E_T - E_P} - \frac{k_4 Q E_P}{K_{mp} + E_P} - k_5[E_P(C_T - X) - K_d X] \tag{6.27}$$

$$\frac{dX}{dt} = k_5[E_P(C_T - X) - K_d X] \tag{6.28}$$

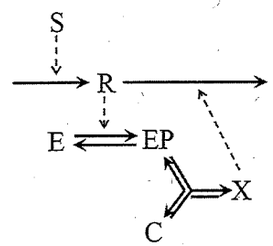

Figure 6.17 A negative feedback oscillator. Wiring diagram.

where $E_T = E + E_P$ is the total concentration of the APC, Q is the (fixed) concentration of a phosphatase, and $C_T = C + X$ is the total concentration of Cdc20. Having left the familiar territory of two-variable systems and phase plane portraits, we must now rely on numerical and qualitative results.

Table 6.2 Parameter values for the delayed negative feedback oscillator.

Parameter	Description	Value	Units
k_1	1^{st}-order rate const	1	min^{-1}
k_2	2^{nd}-order rate const	1	$nM^{-1}min^{-1}$
k_3	1^{st}-order rate const	1	min^{-1}
k_4	1^{st}-order rate const	1	min^{-1}
k_5	2^{nd}-order rate const	0.01	$nM^{-1}min^{-1}$
K_{mk}	Michaelis constant	1	nM
K_{mp}	Michaelis constant	1	nM
K_d	Equilibrium constant	50	nM
S	Signal	0.3	nM
Q	Phosphatase concen.	100	nM
E_T	Total APC concen.	100	nM
C_T	Total Cdc20 concen.	1	nM

Using the parameter values in table 6.2 and S as the control parameter, we can compute a one-parameter bifurcation diagram (figure 6.18a) using numerical tools. In this case, there are two critical values of S at which the system undergoes Hopf bifurcations, with oscillatory solutions in between, $0.2 < S < 0.4$ (roughly). A typical oscillation for S in this range is plotted in figure 6.18b.

Small amplitude oscillations due to a "pure" negative feedback loop have recently been observed by Pomerening et al. (2005) in frog egg extracts (see box 6.6). A long negative feedback loop on PER-protein synthesis seems to play a major role in circadian rhythms, as described in chapter 2.

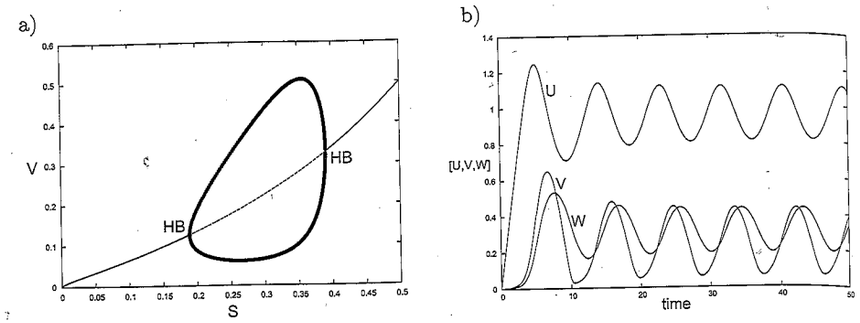

Figure 6.18 A negative feedback oscillator. a) One parameter bifurcation diagram. b) Simulation for $S = 0.3$. See table 6.2 for parameter values. Definitions: $u = R/Q$, $v = E_P/E_T$, $w = X/C_T$. In a), the min and max values of v on the limit cycle oscillation are plotted in the region between the two Hopf bifurcations.

Box 6.6: Negative feedback oscillations in frog egg extracts
Frog egg extracts are convenient preparations in which to observe the negative feedback loop involving MPF and APC, although the native regulatory system also includes a substrate-depletion oscillator involving phosphorylation of MPF (see table 6.1). By clever experimental techniques, Pomerening et al. (2005) have knocked out the substrate-depletion oscillator in a frog egg extract, revealing the negative feedback oscillator in its (presumably) unadulterated state. They observed "pure" negative feedback oscillations in their preparations. In the absence of the self-amplification of MPF activity provided by the substrate-depletion motif, the pure negative feedback oscillations are of considerably smaller amplitude and drive ambiguous transitions into and out of mitosis. It seems that the positive feedback mechanism is important to amplify the negative feedback oscillations and give unambiguous signals to nuclei to enter and leave mitosis.

6.6 A Multiple-Feedback Network: p53 and Mdm2

Transcriptional activator p53 is involved in cell cycle arrest and *apoptosis* (programmed cell death). In normal cells, the level of p53 is kept low by Mdm2, which promotes degradation of p53. The transcription of Mdm2 is activated by p53, creating a negative feedback loop (p53 → Mdm2 —| p53). When a cell is subjected to environmental stress causing DNA damage or oncogene activation, the activity of Mdm2 is weakened, allowing accumulation of p53 in the nucleus. Recently, it has been observed (Lahav et al., 2004) that p53 and Mdm2 undergo one or more oscillations in response to ionizing radiation (which causes double-stranded breaks of DNA), in an apparent attempt to repair the damage. Ciliberto et al. (2005) have proposed a simple mechanism (figure 6.1), including both negative and positive feedback, which quantitatively reproduces this behavior. The equations for the network in figure 6.1 are

$$\frac{d[\mathrm{p53}]}{dt} = k_{s53} - k'_{d53}[\mathrm{p53}] - k_f[\mathrm{Mdm2_{nuc}}][\mathrm{p53}] + k_r[\mathrm{p53U}] \tag{6.29}$$

$$\frac{d[\mathrm{p53U}]}{dt} = k_f[\mathrm{Mdm2_{nuc}}][\mathrm{p53}] - k_r[\mathrm{p53U}] - k'_{d53}[\mathrm{p53U}] - k_f[\mathrm{Mdm2_{nuc}}][\mathrm{p53U}] + k_r[\mathrm{p53UU}] \tag{6.30}$$

$$\frac{d[\mathrm{p53UU}]}{dt} = k_f[\mathrm{Mdm2_{nuc}}][\mathrm{p53U}] - k_r[\mathrm{p53UU}] - (k'_{d53} + k_{d53})[\mathrm{p53UU}] \tag{6.31}$$

$$\frac{d[\mathrm{Mdm2_{cyt}}]}{dt} = k'_{s2} + \frac{k_{s2}[\mathrm{p53_{tot}}]^m}{J_{s2}^m + [\mathrm{p53_{tot}}]^m} - k'_{d2}[\mathrm{Mdm2_{cyt}}] - \frac{k_{ph}}{J_{ph} + [\mathrm{p53_{tot}}]}[\mathrm{Mdm2_{cyt}}] + k_{deph}[\mathrm{Mdm2P_{cyt}}] \tag{6.32}$$

$$\frac{d[\mathrm{Mdm2P_{cyt}}]}{dt} = \frac{k_{ph}}{J_{ph} + [\mathrm{p53_{tot}}]}[\mathrm{Mdm2_{cyt}}] - k'_{d2}[\mathrm{Mdm2P_{cyt}}] - k_{deph}[\mathrm{Mdm2P_{cyt}}] - k_i[\mathrm{Mdm2P_{cyt}}] + k_o[\mathrm{Mdm2_{nuc}}] \tag{6.33}$$

$$\frac{d[\mathrm{Mdm2_{nuc}}]}{dt} = V_{ratio}(k_i[\mathrm{Mdm2P_{cyt}}] - k_o[\mathrm{Mdm2_{nuc}}]) - k_{d2}[\mathrm{Mdm2_{nuc}}] \tag{6.34}$$

$$\frac{d[\mathrm{DNA_{dam}}]}{dt} = k_{dam}[\mathrm{IR}] - k_{rep}[\mathrm{p53_{tot}}]\frac{[\mathrm{DNA_{dam}}]}{J_{dna} + [\mathrm{DNA_{dam}}]} \tag{6.35}$$

where

$$k_{d2} = k'_{d2} + \frac{[\mathrm{DNA_{dam}}]}{J_{dam} + [\mathrm{DNA_{dam}}]}k''_{d2} \tag{6.36}$$

$$[\mathrm{p53_{tot}}] = [\mathrm{p53}] + [\mathrm{p53U}] + [\mathrm{p53UU}] \tag{6.37}$$

$$[\mathrm{Mdm2_{tot}}] = [\mathrm{Mdm2_{cyt}}] + [\mathrm{Mdm2P_{cyt}}] + \frac{1}{V_{ratio}}[\mathrm{Mdm2_{nuc}}] \tag{6.38}$$

$$V_{ratio} = \frac{V_{cytoplasm}}{V_{nucleus}} \tag{6.39}$$

$$[\mathrm{IR}] = \text{imposed dose of ionizing radiation} \tag{6.40}$$

The network contains a long negative feedback loop (p53 → $\mathrm{Mdm2_{cyt}}$ → $\mathrm{Mdm2P_{cyt}}$ → $\mathrm{Mdm2_{nuc}}$ —| p53) and a long positive feedback loop (p53 → PTEN —| PIP3 → Akt → $\mathrm{Mdm2P_{cyt}}$ → $\mathrm{Mdm2_{nuc}}$ —| p53). The positive feedback loop is shortened to p53 —| $\mathrm{Mdm2P_{cyt}}$ → $\mathrm{Mdm2_{nuc}}$ —| p53.

A simulation of this network (figure 6.19) compares very favorably with the experimental observations of (Lahav et al., 2004). As the radiation dose increases (figure 6.19d), the number of pulses of p53 increases. The reason for this curious "digital" response of p53 to DNA damage is made clear by the one-parameter bifurcation diagram in figure 6.20, where we plot system response, $[\mathrm{p53_{tot}}]$, as a function of the extent of DNA damage, measured by k_{d2}. The positive feedback

Table 6.3 Parameter values for p53-Mdm2 network

Rate Constants (min^{-1})		
$k_{s53} = 0.055$	$k'_{d53} = 0.0055$	$k_{d53} = 8$
$k_f = 8.8$	$k_r = 2.5$	$k'_{s2} = 0.0015$
$k_{s2} = 0.006$	$k'_{d2} = 0.01$	$k''_{d2} = 0.01$
$k_{ph} = 0.05$	$k_{deph} = 6$	$k_i = 14$
$k_0 = 0.5$	$k_{dam} = 0.18$	$k_{rep} = 0.017$

Other Constants (dimensionless)		
$J_{s2} = 1.2$	$J_{ph} = 0.01$	$J_{dna} = 1$
$J_{dam} = 0.2$	$V_{ratio} = 15$	$m = 3$

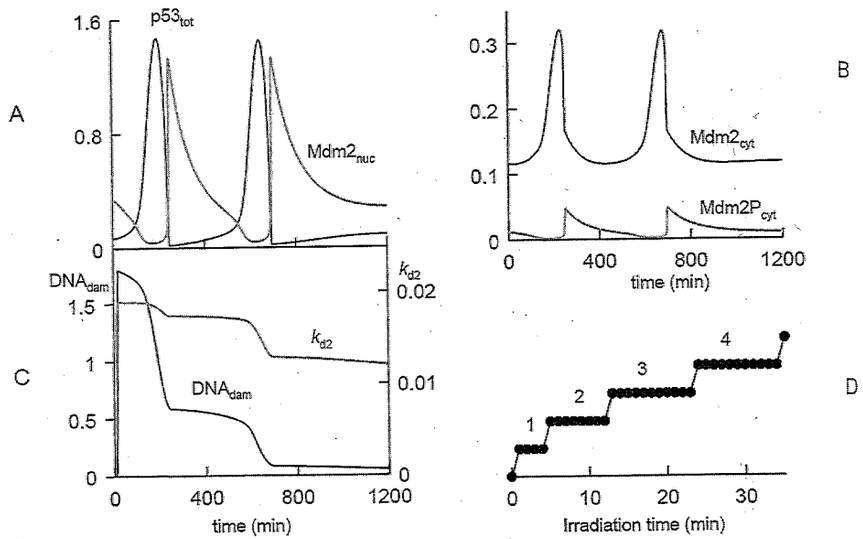

Figure 6.19 Simulation of gamma-irradiation experiment (reproduced from (Ciliberto et al., 2005), with permission). At the beginning of the simulation, the system is at steady state. (A) Between time 10 and 20, the control system is exposed to a transient damaging agent, which induces two large amplitude oscillations in $p53_{tot}$ and Mdm2nuc. (B) The oscillations of the two cytoplasmic forms of Mdm2 have a smaller amplitude compared to $Mdm2_{nuc}$ concentration in panel (A). (C) The oscillations are initiated as a consequence of k_{d2} increase, which is induced by irradiation. As the damage is repaired, k_{d2} decreases back to its basal value. (D) The number of pulses increases with the amount of damage. In the simulation, we count the number of oscillations as a function of the irradiation time. In panels A through C irradiation time = 10 min.

in the network creates multiple steady states (the S-shaped curve at $k_{d2} \cong 0.01$), but the negative feedback loop makes the upper steady state unstable. The unstable upper steady state is surrounded by stable limit cycle oscillations of $[p53_{tot}]$ and $[Mdm2_{tot}]$. The region of stable oscillation is bounded above (at $k_{d2} \cong 0.853$) by a Hopf bifurcation, and below (at $k_{d2} \cong 0.0135$) by a saddle-node-loop bifurcation. For a broad range of values of k_{d2}, that is, of DNA damage, the system responds with pulses of p53 and Mdm2 of fixed amplitude and period, exactly as observed by Lahav et al. (2004). As the damage is repaired, k_{d2} drops toward $k_{d2} \cong 0.01$, and the oscillations disappear abruptly as k_{d2} crosses the saddle-node-loop bifurcation point.

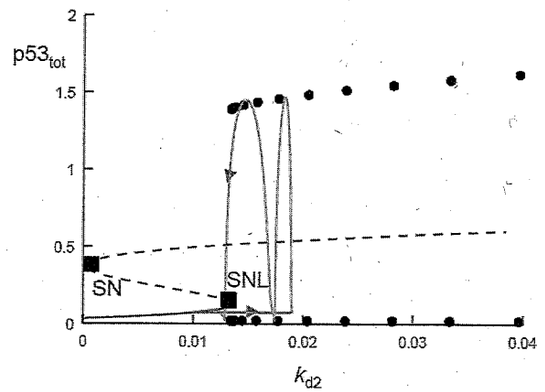

Figure 6.20 Bifurcation diagram (reproduced from (Ciliberto et al., 2005), with permission). Recurrent states (steady states and limit cycles) for $p53_{tot}$ are plotted as functions of k_{d2}, the degradation rate of $Mdm2_{nuc}$. The solid line represents stable steady states, the dotted line unstable steady states. Black dots are the maxima and minima of the stable limit cycles. The grey solid line represents $p53_{tot}$ as a function of k_{d2} from the simulation shown in figure 6.19. Notice that in figure 6.19 k_{d2} is a variable (see equations), while here it is a parameter (all other equations and parameter values as in table 6.3). When the qualitative behavior of the system changes, it is said to undergo a bifurcation. In the p53/Mdm2 model there is a saddle-node (SN) bifurcation at k_{d2}=0.0018 and a saddle-node-loop (SNL) bifurcation at k_{d2}=0.0135. Before the SNL bifurcation there is only one stable steady state, with low p53 ("p53 OFF"); after the SNL the steady state becomes unstable, surrounded by a stable limit cycle. The family of stable limit cycles disappears at a Hopf bifurcation at k_{d2} =0.8532 (not shown on the diagram).

A somewhat different model of p53/Mdm2 oscillations in response to ionizing radiation has recently been published by (Ma et al., 2005).

6.7 Conclusions

How are cell biologists to make reliable connections between molecular interaction networks and cell behaviors, when intuition fails in all but the simplest cases? In this chapter, we propose to make the connection by translating the reaction network into a set of nonlinear differential equations that describe how all the interacting species are changing with time (figure 6.21).

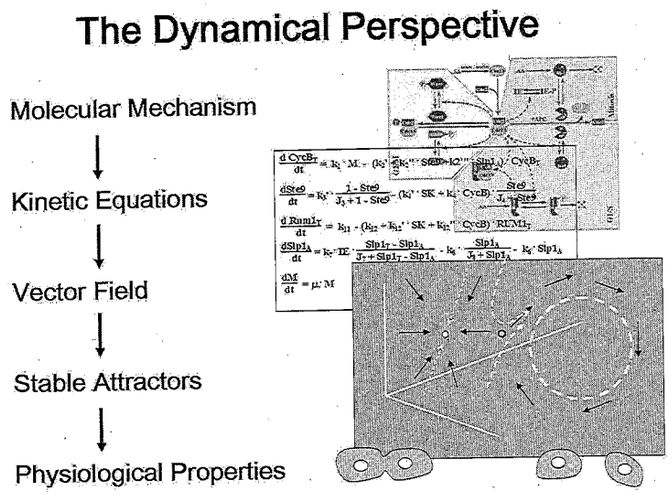

Figure 6.21 A dynamical perspective on molecular cell biology. To make a connection between molecular mechanisms and cell physiology, we convert the mechanism into a set of kinetic equations, by standard principles of biochemical kinetics, and view the kinetic equations as defining a vector field in the state space of the dynamical variables. The vector field has attracting solutions (steady states and oscillations) that correspond to characteristic physiological responses of the cell. The dependence of these attractors on kinetic constants (hence, on genetics and environment) are robustly captured in bifurcation diagrams.

The differential equations define a vector field in the state space of the network. The vector field points to certain stable attractors, which can be correlated with long-term, stable behavior of the network and of the cell it governs. Transitions from one stable attractor to another represent the responses of the cell to specific perturbations (signals). A natural way to describe the signal-response properties of a regulatory network is in terms of a one-parameter bifurcation diagram, which efficiently displays the stable attractors (steady states and oscillators) and transitions between attractors as signal strength (the "parameter") varies.

We have illustrated these ideas with simple examples of linear, hyperbolic, and sigmoidal signal-response curves, of bistable switches based on positive feedback

or mutual inhibition, and of limit cycle oscillators based on substrate depletion, activator-inhibitor interactions, or time-delayed negative feedback. These fundamental motifs (switches and oscillations) can be coupled together into networks of increasing complexity and dynamical potential. Interested readers should now be ready to read and understand the growing body of literature that takes this dynamical perspective on interesting topics in cell physiology. Some nice examples include: cell-cycle control (Tyson et al., 2002), circadian rhythms (Leloup and Goldbeter, 1998), lysogenic viruses (Arkin et al., 1998), quorum sensing in bacteria (James et al., 2000; Usseglio Viretta and Fussenegger, 2004), NF-κB signaling (Hoffmann et al., 2002), and programmed cell death (Eissing et al., 2004).

biology

Contributors

Benjamin J. Bornstein, Emery Conrad, Hidde de Jong, Francis J. Doyle III, John Doyle, Johan Elf, Andrew Finney, Akira Funahashi, Kapil G. Gadkar, Daniel T. Gillespie, Rudiyanto Gunawan, Michael Hucka, Pablo A. Iglesias, Brian P. Ingalls, Mads Kærn, Sarah M. Keating, Douglas B. Kell, Hiroaki Kitano, Steffen Klamt, Joshua D. Knowles, Ben L. Kovitz, Karsten Kruse, Joanne Matthews, Denis Noble, Johan Paulsson, Vipul Periwal, Linda R. Petzold, Delphine Ropers, Uwe Sauer, Maria J. Schilstra, Bruce E. Shapiro, Jörg Stelling, Zoltan Szallasi, John J. Tyson, Ron Weiss, Tau-Mu Yi

The MIT Press
Massachusetts Institute of Technology
Cambridge, Massachusetts 02142
http://mitpress.mit.edu

0-262-19548-8

System Modeling in Cellular Biology
SZALLASI, STELLING, AND PERIWAL, EDITORS

System Modeling in Cellular Biology

FROM CONCEPTS TO NUTS AND BOLTS

EDITED BY ZOLTAN SZALLASI, JÖRG STELLING, AND VIPUL PERIWAL